Journal of Physics Research and Education, Volume 3, March 2026

The Notion of Age Emerged from the Longitudinal Evolution of Purely Electromagnetic Showers: A Review

Animesh Basak, Meghamani Haldar, Kishor Chaudhury, and Rajat K. Dey*
Department of Physics, University of North Bengal, Siliguri, 734013, WB, India

The state of the longitudinal development of high-energy cosmic-ray air showers has been characterized by the notion of shower age. Moreover, at a given atmospheric level, the shape of the energy spectrum of electrons in a cosmic-ray shower with ultra-high-energy depends only on the shower age at this level. This work is an in-depth review of the conceptual underpinnings of the electromagnetic cascade theory, which extends to Rossi and Greisen's viewpoint as well as to the recently acknowledged quests by others. The structure of this work consists of two parts. In the first part, we review how basic arguments can be used to grasp the properties linked to the shower age. In the second part, we look at how the structures of the electron and photon spectra, as well as the relative normalization corresponding to a particular age, can be known more rationally. As we end our review, we refer to several new concepts derived from recent Monte Carlo shower analyses.

I. INTRODUCTION

Since about 1940, cosmic-ray (CR) research has employed the notion of shower age. It first shows up in Rossi and Greisen's early works [1] and then in Nishimura's work [2]. The concept of longitudinal development in electromagnetic (EM) cascade theory was leveraged in their studies to formulate various expressions required for the solutions of the diffusion equations. In order to solve the diffusion equations in the three-dimensional EM cascade theory, it was applied to the lateral spread of electrons along the cascade axis. Greisen [3] offered one of the most widely used analytical depictions of the average longitudinal profile. The so-called Greisen profile has been derived from Snyder's calculations within the so-called approximation B considering only three processes: (i) pair production by photons (henceforth γ(s)), (ii) bremsstrahlung by electrons (henceforth e(s), stands for either e^- or e^+) and (iii) collision energy loss suffered by e(s). The Greisen profile is given by,

$$N_{\rm Greisen} = \frac{0.31}{\sqrt{\ln(E_0/\epsilon_0)}} \exp[X(1-1.5 \ \ln s)] \tag{1}$$

where s indicates the stage of the longitudinal cascade development, and E_0 is the energy of the primary γ causing the cascade. Here the atmospheric depth X is expressed in cascade units, normalized by the radiation length of e(s) in air, which is equal to 37.1 g cm^{-2}).

The shower age s-parameter is the main way to express the average evolving stage of pure EM cascades. In essence, it is the inverse of the fractional rate of change of the total number e(s) of an

* rkdey2007phy@nbu.ac.in

atmospherically deep extended air shower (EAS) [1]. The size slope $\lambda(s)$ is the name given to the following fractional rate of change:

$$\lambda(s) = \frac{1}{N_{\rm e}(X)} \frac{{\rm d}N_{\rm e}(X)}{{\rm d}X}. \tag{2}$$

Therefore, the parameter s can be described mathematically as the rate of increase and decay of $N_{\rm e}(X)$ in a shower. It is given as,

$$s = {\lambda_1}^{-1}(\lambda(s)) = {\lambda_1}^{-1}\left(\frac{1}{N_{\rm e}(X)} \frac{{\rm d}N_{\rm e}(X)}{{\rm d}X}\right), \tag{3}$$

where λ_1^{-1} describes the inverse function of $\lambda(s)$. The function $\lambda(s)$ continually decreases and has a single zero at $s = 1$; and therefore, according to Eq. (3), showers have age $s = 1$ at the maximum and age $s < 1$ ($s > 1$) before (after) the maximum. Rossi and Greisen provided a more straightforward physical interpretation of s as a shape or spectral index of the energy spectra of secondary EM particles after performing a few mathematical operations on Eq. (2), i.e., by adopting the particular mapping of Eq. (3) between λ and s. The energy spectra of secondary e(s) or γ(s) in a shower induced by a e or a γ follow a power law of the form:

$$n_e(E) \sim n_\gamma(E) \sim E^{-(s+1)}. \tag{4}$$

The power law operates above the critical energy ϵ_0, defined as the energy at which ionization and bremsstrahlung energy losses are the equal for an electron in air, which occurs at $\epsilon_0 \approx 82$ MeV for e(s). These power law characteristics ceases when E approaches (from above) the critical energy of e. For energies below $E \sim \varepsilon$ the spectrum of e(s) has a sharp cutoff, while the spectrum of γ(s) has a 'knee' which obeys E^{-1} variation. It is possible to compute the exact shapes of the cutoff for the e spectrum, the knee of the γ spectrum (i.e., the change from the form $E^{-(s+1)}$ to E^{-1}), and the relative normalizations of the γ and e spectra. All of these shapes are completely determined by s (alternatively, by the size slope λ).

The concept of shower age for showers produced by ultra high energy (UHE) CRs in the Earth's atmosphere has been re-examined in a few recent research [4–6]. Using Monte Carlo (MC) techniques, Giller *et al.* [4] and Nerling *et al.* [5] investigated the showers produced in air by high energy protons (p) and nuclei. They found that the energy and angle distributions of the e(s) in the showers have shapes that, to a good approximation, are only determined by the parameter $\overline{s}$, defined as:

$$\overline{s}(X, X_{\rm max}) = \frac{3\,X}{X + 2\,X_{\rm max}}\,, \tag{5}$$

where the depth at which the shower reaches its greatest size is denoted by $X_{\rm max}$. The shower size $N_{\rm e}$, which essentially corresponds to the electron size, is defined as the total number of charged particles integrated over all energies. Gora *et al.* [6] have extended these findings to the lateral distribution of e(s). It is therefore desirable to acquire a fuller knowledge of the genesis and limitations of this attribute of 'universality', which is quite significant for the analysis and interpretation of high energy CR findings. Since the widely accepted definition of age in Eq. (5) always matches the general definition [Eq. (3)] at $X_{\rm max}$, it is a fairly accurate estimate for showers that are close enough to the maximum. The rationale behind the broader definition would seem to be a formal 'principle' question. In fact, the general definition provides the proper s in several situations where the two definitions differ dramatically. Only for a specific shower longitudinal shape, known as the 'Greisen profile' [3–7], does the definition given in Eq. (5) match the proper one. The Greisen profile and the age definition given in Eq. (1) are actually closely related, and they can be viewed as the integral and derivative of one another (via the mediation of the function λ_1). Although, it is merely a rough approximation for the description of individual hadronic showers, the Greisen profile (described above) accurately characterizes the average development of solely EM showers. The variation of a shower profile from the Greisen profile with the same $X_{\max}$ is of the same order as the deviation of the definition in Eq. (5) from the true age, defined in Eq. (3).

The average longitudinal evolution of exclusively EM EASs is reviewed in the following, first in 'approximation A' (henceforth Approx. A), which ignores the ionization losses by e(s), and subsequently in 'approximation B' (henceforth Approx. B). In this research, the idea of age arose naturally. The 'universal spectra' of showers of age s correspond to the elementary solutions of the shower equations in Approx. B, which are denoted by the parameter s. The popular 'Greisen profile', which characterizes the typical longitudinal development of solely EM showers, is covered in the following section. Lastly, we make some conclusions.

II. ELECTROMAGNETIC SHOWERS IN APPROX. A

Two sets of simplifying assumptions known as 'Approx. A' and 'Approx. B' are used to study the evolution of the EM, i.e. γ- or e-initiated showers [1]. Pair generation for γ(s) and bremsstrahlung for e(s) are the only processes taken into account for the shower development in Approx. A. Asymptotic formulae valid at high energy characterize the differential cross sections for these processes. The energy losses by e(s) resulting from collisions with the nuclei of the medium and e(s) are ignored. The functions $n_e(E, X)$ and $n_\gamma(E, X)$, which provide the differential energy spectra of e(s) and γ(s) at depth X, explain the average longitudinal evolution of EM showers. Although Rossi and Greisen's nomenclature as illustrated in [1], is used in this study, we use new symbols. Rossi and Greisen designated the γ spectrum as $\gamma(E, X)$ and the differential (integral) e spectrum as $\pi(E, X)$ ($\Pi(E, X)$); the subscript notation employed here is more appropriate for extending the approach to hadronic showers when various nucleon/nuclei types are present. The following two integro–differential equations in Approx. A illustrate how the e and γ differential spectra evolve:

$$\begin{aligned}\frac{\partial n_e(E,X)}{\partial X} &= -\int_0^1 dv\,\varphi_0(v)\left[n_e(E,X) - \frac{1}{1-v}n_e\left(\frac{E}{1-v},X\right)\right] \\ &+ 2\int_0^1 \frac{du}{u}\,\psi(u)\,n_\gamma\left(\frac{E}{u},X\right)\end{aligned} \tag{6}$$

$$\frac{\partial n_\gamma(E,X)}{\partial X} = \int \times_0^1 \frac{dv}{v}\,\varphi(v)\,n_e\left(\frac{E}{v},X\right) - \sigma_0\,n_\gamma(E,X). \tag{7}$$

The $(e \to e)$ contribution and the $(\gamma \to e)$ processes are described respectively by the first and second terms on the right side of Eq. (6). The $(e \to \gamma)$ contribution and the γ absorption are described respectively by the first and second terms on the right side of Eq. (7). The γ absorption cross section and the differential cross sections for pair formation and bremsstrahlung can be found in [1].

A. Basic solutions

There is no energy scale in the system of Eqs. (6) and (7). As a result, these equations have a set of scale-invariant 'primary' solutions of the following form:

$$\begin{cases} n_e(E,X) = K\,E^{-(s+1)}e^{\lambda(s)X} \\ n_\gamma(E,X) = K\,r_\gamma(s)\,E^{-(s+1)}e^{\lambda(s)X}. \end{cases} \tag{8}$$

The solutions vary exponentially with depth X and exhibit power law in energy. One derives a quadratic equation for $\lambda(s)$ with two solutions by inserting these answers into the shower Eqs. (6) and (7):

$$\lambda_{1,2}(s) = -\frac{1}{2}\,(A(s)+\sigma_0) \pm \frac{1}{2}\sqrt{(A(s)-\sigma_0)^2 + 4\,B(s)\,C(s)}. \tag{9}$$

There is a γ/e ratio associated with each solution:

$$r_\gamma^{(1,2)}(s) = \frac{C(s)}{\sigma_0 + \lambda_{1,2}(s)}. \tag{10}$$

The auxiliary functions $A(s)$, $B(s)$ and $C(s)$ appeared in Eq. (9) and Eq. (10) are explicitly provided in [8].

It is highly helpful to follow Greisen [1] and introduce the nearly exact and equivalent simplified expression (deviations fewer than 2% in the interval $0.6 \leqslant s \leqslant 1.4$) even if $\lambda_1(s)$ is already given by an explicit analytic expression:

$$\overline{\lambda}_1(s) = \frac{1}{2}\,(s - 1 - 3\,\ln s)\,. \tag{11}$$

It is physically easy to see that there are two solutions $\lambda_{1,2}(s)$ for each value of s. The spectra maintain the same power law shapes at all X, but their relative and absolute normalizations alter if one begins at $X = 0$ with populations of e(s) that have a power law form with the same slope but arbitrary normalizations. After reaching an asymptotic γ/e ratio with a X scale $|\lambda_2(s)|^{-1}$, the spectra evolve exponentially $\propto e^{\lambda_1(s)\cdot X}$ while maintaining a constant equilibrium ratio. Since $|\lambda_2(s)| > |\lambda_1(s)|$ for all s values, the fastest process is the convergence to an asymptotic γ/e ratio. An initial power law, pure e spectrum, for instance:

$$\begin{cases} n_e(E,0) \;=\; K\;E^{-(s+1)} \\ n_\gamma(E,0) \;=\; 0 \end{cases} \tag{12}$$

evolves in X as:

$$\begin{cases} n_e(E,X) \;=\; \frac{K}{\lambda_1(s)-\lambda_2(s)}\;\left[(\lambda_1(s)+\sigma_0)\,e^{\lambda_1(s)\,X} - (\lambda_2(s)+\sigma_0)\,e^{\lambda_2(s)\,X}\right]\;E^{-(s+1)} \\ n_\gamma(E,X) \;=\; \frac{K}{\lambda_1(s)-\lambda_2(s)}\;C(s)\;\left[e^{\lambda_1(s)\,X} - e^{\lambda_2(s)\,X}\right]\;E^{-(s+1)} \end{cases}. \tag{13}$$

For every value of X, the spectra continue to be power laws. The spectra evolve in X as a simple exponential ($\propto e^{\lambda_1(s)\cdot X}$) with an asymptotic γ/e ratio $C(s)/(\lambda_1(s)+\sigma_0)$ that corresponds to the first solution in Eq. (10) for $X \gg |\lambda_2(s)|^{-1}$ if $e^{\lambda_2(s)X}$ is set to zero. In the end, any combinations of γ and e spectra power laws of the same slope s 'converge' to the solutions, which are a kind of 'attractor'

$$\begin{cases} n_e(E,X) = K' E^{-(s+1)} e^{\lambda_1(s)X}, \\ n_\gamma(E,0) = K' E^{-(s+1)} e^{\lambda_1(s)X}\, r_\gamma^{(1)}(s). \end{cases} \tag{14}$$

One particular X independent solution, which is especially significant, relates to $s = 1$. The existence of this X–independent solution:

$$\begin{cases} n_e(E,X) \;=\; K\; E^{-2} \\ n_\gamma(E,X) \;=\; K\; \overline{r}_\gamma\; E^{-2} \end{cases} \tag{15}$$

and its energy dependence $\propto E^{-2}$ do not depend on the specific form of the bremsstrahlung and pair production cross sections. This can be easily understood by noting that the bremsstrahlung and pair production processes that 'mix' the e and γ populations conserve energy and are scale invariant, and that a power law spectrum of the form E^{-2} contains an equal amount of energy in each energy decade. The exact shape of the cross sections determines only the value of the γ/e ratio that corresponds to the solution:

$$\overline{r}_\gamma = r_\gamma^{(1)}(1) = \frac{\langle v\rangle_{\rm brems}}{\sigma_0} = \frac{C(1)}{\sigma_0} = \frac{(1+b)}{(7/9 - b/3)} \simeq 1.31. \tag{16}$$

The fact that $\lambda_1(s)$ is positive for $s < 1$ and negative for $s > 1$ is also independent of the detailed form of the cross sections. This is a straightforward result of the energy contained in each decade in a power law spectrum of form $E^{-(s+1)}$ increasing with E when $s < 1$, and decreasing when $s > 1$. Additionally, this simple description already shows how the structure of the particle energy spectra in an EAS is closely linked to the X–dependence of the shower development.

B. Showers generated by a primary γ or $e^{\pm}$

Rossi and Greisen [1] estimated the development of the shower produced by a primary e or γ of initial energy E_0, in Approx. A. Prior to providing a detailed description of these solutions, we might note that certain significant characteristics can be easily inferred from straightforward considerations. The solutions' differential spectra of e(s) and γ(s) have the scaling nature:

$$n_\alpha(E_0,E,X) = \frac{1}{E_0}\, f_\alpha\left(\frac{E}{E_0}, X\right) \tag{17}$$

(the subscript α runs over the four situations: $e \to e$, $e \to \gamma$, $\gamma \to e$ and $\gamma \to \gamma$). Correspondingly, the integral spectra have the scaling form:

$$N_\alpha(E_0,E_{\min},X) = \int_{E_{\min}}^{E_0} dE\; n_\alpha(E_0,E,X) = F_\alpha\left(\frac{E_{\min}}{E_0}, X\right) . \tag{18}$$

The lack of quantities having the dimension of energy in the shower equations leads to these scaling features of the Approx. A solutions. The following condition reflects energy conservation:

$$\int_0^{E_0} dE\; E\; n_e(E_0, E, X) + \int_0^{E_0} dE\; E\; n_\gamma(E_0, E, X) = E_0. \tag{19}$$

The solution of the cascade equations for a monochromatic γ or e [1] is quite easier for the Mellin transforms of functions n_e and n_γ. These transformations can then be reversed to give the physically observable spectrum. With a single path integration along a line in the complex plane, the inversion can be accomplished numerically with ease and correct results. Additionally, Rossi and Greisen have demonstrated that the transform may be inverted using a 'saddle point approximation', yielding straightforward formulas for the spectra that are both amazingly precise and highly instructive.

The saddle point approximation solutions for the differential spectra (valid for much larger X and $E/E_0 \ll 1$) follow:

$$n_\alpha(E_0, E, X) \simeq \frac{1}{E_0}\,\frac{1}{\sqrt{2\pi}}\left[\frac{G_\alpha(s)}{\sqrt{\lambda_1''(s)\,X}}\left(\frac{E}{E_0}\right)^{-(s+1)} e^{\lambda_1(s)\,X}\right]_{s=\bar{s}(E/E_0, X)} \tag{20}$$

along with

$$\bar{s}\left(\frac{E}{E_0}, X\right) \simeq \frac{3X}{X - 2\ln(E/E_0)}\,. \tag{21}$$

The saddle point approximation solution for the integral spectra is

$$N_\alpha(E_0, E_{\min}, X) \simeq \frac{1}{\sqrt{2\pi}}\left[\frac{1}{s}\,\frac{G_\alpha(s)}{\sqrt{\lambda_1''(s)\,X}}\left(\frac{E_{\min}}{E_0}\right)^{-s} e^{\lambda_1(s)\,X}\right]_{s=\bar{s}(E_{\min}/E_0, X)}. \tag{22}$$

Consider that for $E_{\min} \to 0$, both the e and γ integral spectra diverge. A derivation of these well-known results can be found in [1, 8] for completeness.

Several intriguing characteristics are displayed by the saddle point solutions of the shower equations in Approx. A:

- The differential and integral spectra for a fixed value (< 1) of the ratio E/E_0 (or $E_{\min}/E_0$) begin at zero for $X \simeq 0$, rise with increasing X, reach a maximum at the value $X_{\max}$, and then start to diminish and vanish for $X \to \infty$. The X evolution of the solution is governed by the exponential factor $e^{\lambda_1(s)\,X}$. Consequently, the shower maximum roughly corresponds to $\lambda_1(s) = 0$ (and so to $s = 1$). Equation (21) yields the well-known result:

$$X_{\max}\left(\frac{E}{E_0}\right) \simeq \ln\left(\frac{E_0}{E}\right). \tag{23}$$

Equation (21) can therefore be rewritten as,

$$\bar{s}\left(\frac{E}{E_0}, X\right) \simeq \frac{3X}{X + 2\,X_{\max}}\,. \tag{24}$$

- More generally, since the X dependence of the solution is controlled by the component $e^{\lambda_1(s)\,X}$, it follows that, to a decent approximation, one has:

$$\frac{1}{N_\alpha}\frac{\partial N_\alpha}{\partial X} \simeq \lambda_1\left[\overline{s}\left(\frac{E_{\min}}{E_0}, X\right)\right] \text{ or } \frac{1}{n_\alpha}\frac{\partial n_\alpha}{\partial X} \simeq \lambda_1\left[\overline{s}\left(\frac{E}{E_0}, X\right)\right]. \tag{25}$$

- The structure of the energy spectrum around E is correlated with the quantity $\overline{s}(E/E_0, X)$, which clearly represents the spectrum's 'local slope' at energy E:

$$-\frac{E}{n_\alpha}\frac{\partial n_\alpha}{\partial E} \simeq \overline{s}\left(\frac{E}{E_0}, X\right) + 1. \tag{26}$$

  Taken another way, the spectrum around E can be roughly represented as a power law $E^{-(\overline{s}+1)}$. The spectrum is not a straightforward power law globally, and the 'local slope' varies with E/E_0 and X. The local slope $\overline{s}$ increases monotonically with E/E_0 for a fixed depth X as the spectrum gets steeper. The spectrum also gets steeper as X increases and the local slope grows monotonically for a fixed value of E/E_0. When the spectrum for energy E reaches its maximum level, it takes the form $\propto E^{-2}$.

- The γ/e ratio varies slowly with energy because the spectra of γ(s) and e(s) have extremely similar but distinct forms. One may determine the following from the expressions for the functions $G_\alpha(s)$ in [1, 8]:

$$\frac{n_\gamma(E_0, E, X)}{n_e(E_0, E, X)} \simeq \frac{C(\overline{s})}{\sigma_0 + \lambda_1(\overline{s})} = r_\gamma^{(1)}(\overline{s}) \tag{27}$$

  For the elementary power law solution with slope $s = \overline{s}(E/E_0, X)$, that is the 'asymptotic ratio'. It is noteworthy that this consequence is unaffected by the type of particle (γ or e) that starts the shower.

- The secondary e and γ populations rapidly tend to attain a form of dynamic equilibrium feeding each other, as evidenced by the unexpectedly close developments of showers started by a γ or a e of the same energy.

The equations in Approx. A make it impossible to naturally link a particular age to a shower since they have no significant energy scale (apart from the main particle's energy). Consequently, according to Eq. (21), each ratio E/E_0 (or $E_{\min}/E_0$) can be associated with a distinct age for a given depth X. The age parameter $\overline{s}$ simultaneously characterizes the shape of the spectrum at energy E, which is well represented by the power law $\propto E^{-(\overline{s}+1)}$, and the 'stage' of the longitudinal evolution of the spectrum by Eq. (25). Equation (27) states that the γ/e ratio around E is similarly controlled by the age.

III. ELECTROMAGNETIC SHOWERS IN APPROX. B

The energy losses of e(s) are simply represented in Approx. B as an energy independent loss ε per unit of radiation length. The critical energy is represented by the amount ε, which is approximately 81 MeV in air. As a result, a term that characterizes the evolution of e is added to the right side of Eq. (6):

$$\begin{aligned} \frac{\partial n_e(E,X)}{\partial X} &= -\int_0^1 dv\ \ \varphi_0(v)\ \left[n_e(E,X) - \frac{1}{1-v}\, n_e\left(\frac{E}{1-v}, X\right)\right] \\ &+2\int_0^1 \frac{du}{u}\,\psi(u)\, n_\gamma\left(\frac{E}{u}, X\right) + \varepsilon\,\frac{\partial n_e(E,X)}{\partial E}. \end{aligned} \tag{28}$$

There are no more straightforward power law solutions of the form Eq. (9) for the new system of Eq. (29) and Eq. (8). Even so, it is possible to introduce 'elementary' solutions with a constant energy form and evolve with X, and exhibit the straightforward behavior $e^{\lambda(s)\,X}$. The elementary answers, according to Rossi and Greisen [1], can be expressed as follows:

$$\begin{cases} n_e(E,X) \ = \ K\ \ e^{\lambda(s)\,X}\ E^{-(s+1)}\ p\left(s, \frac{E}{\varepsilon}\right) \\ n_\gamma(E,X) \ = \ K\ e^{\lambda(s)\,X}\ E^{-(s+1)}\ g\left(s, \frac{E}{\varepsilon}\right)\ r_\gamma(s) \end{cases} \tag{29}$$

These have two extra functions, $p(s,x)$ and $g(s,x)$. The collision losses of e(s) can be safely ignored for large energy ($E \gg \varepsilon$), and the solutions match the straightforward power law form of Approx. A. According to this restriction, the functions $\lambda(s)$ and $r_\gamma(s)$ that occur in Eq. (29) match with the functions previously discussed and provided in Eq. (9) and Eq. (10), and the functions $p(s,x)$ and $g(s,x)$ asymptotically become unity for large E/ε:

$$\lim_{x\to\infty} p(s,x) = 1, \qquad \lim_{x\to\infty} g(s,x) = 1. \tag{30}$$

Substituting Eq. (29) into the shower equations, one may obtain two pairs of integro-differential equations for the functions $p(s,x)$ and $g(s,x)$ related to the two solutions for $\lambda(s)$ [1, 8]. The functions $p_{1,2}(s,x)$ and $g_{1,2}(s,x)$ can be obtained by numerically solving these equations.

The functions $p_1(s,x)$ and $g_1(s,x)$ have transparent physical meanings. If one injects power laws spectra of e(s) and γ(s) of the form $E^{-(s+1)}$ after a few lengths $|\lambda_2(s)|^{-1}$, the spectra take asymptotically constant shapes given by

$$\begin{cases} n_e(E,X) \ = \ K\ \ e^{\lambda_1(s)\,X}\ E^{-(s+1)}\ p_1\left(s, \frac{E}{\varepsilon}\right) \\ n_\gamma(E,X) \ = \ K\ e^{\lambda_1(s)\,X}\ E^{-(s+1)}\ g_1\left(s, \frac{E}{\varepsilon}\right)\ r_\gamma^{(1)}(s) \end{cases} \tag{31}$$

(the same as Eq. (29), but choosing the first of the two potential solutions) and proceed to evolve in X as a conventional exponential. This asymptotic solution's qualitative characteristics are simple to comprehend. When e(s) are absorbed due to ionization losses, the e spectrum has a cutoff for $E \sim \varepsilon$, but normally it is a nearly perfect power law for $E \gg \varepsilon$. The $1/E$ dependency of the bremsstrahlung cross section is reflected in the γ spectrum, that changes from a power law $\propto E^{-(s+1)}$ for $E \gg \varepsilon$ to the form $\propto E^{-1}$ for $E \ll \varepsilon$. The explicit calculation initially carried out by Rossi and Greisen [1] confirms these physically intuitive qualities. They show that the behavior of the functions $p(s,x)$ and $g(s,x)$ for $x \to 0$ is:

$$p(s,x) \propto x^{s+1} \quad \text{and} \quad g(s,x) \propto x^{s}. \tag{32}$$

The e spectrum approaches a finite value for $E \to 0$, according to the low energy behavior of the function $p(s,x)$. As a result, the e spectrum's energy integration converges for both $E \to \infty$ (if $s > 0$) and $E \to 0$, making it feasible to discuss the N_{e}. The integral spectrum diverges logarithmically at the lower limit, as the expected differential photon spectrum diverges $\propto E^{-1}$ for $E \to 0$. For the phenomenologically most significant solution (corresponding to $\lambda_1(s)$), the N_{e} can be expressed as,

$$N_e(s) = \int_0^\infty dE\, n_e(E) \;\propto\; \int_0^\infty dE\, E^{-(s+1)}\, p_1\left(s, \frac{E}{\varepsilon}\right)$$
$$= \varepsilon^{-s} \int_0^\infty dx\, x^{-(s+1)}\, p_1(s,x) = \varepsilon^{-s}\, \frac{K_1(s,-s)}{s}. \tag{33}$$

The last equation characterizes the function $K_1(s,-s)$. The phyical essence of $K_1(s,-s)$ can be understood comparing Eq. (33) with the integral:

$$\int_\varepsilon^\infty dE\, E^{-(s+1)} = \frac{\varepsilon^{-s}}{s}.$$

The integration of the simple form $E^{-(s+1)}$ in the range $(\varepsilon \leqslant E \leqslant \infty)$ differs from the N_{e} obtained by integrating over all E the elementary solution (Eq. (29)) by a factor $K_1(s,-s)$. For any integer values $s \geqslant 0$, Rossi and Greisen have demonstrated how to compute the exact values of the function $K_1(s,-s)$. Numerical techniques can be used to determine the functions $p_{1,2}(s,x)$ and $g_{1,2}(s,x)$ [8]. The functions can alternatively be expressed as power expansions in $1/x$ with readily available coefficients for $x > 1$ [1]. For three values of the index s, Figs. 1 and 2 illustrate the behavior of the e spectrum as $dn_e/d\ln E = En_e(E)$ (on a linear and log scale). Particles in the energy range $0.01 \lesssim E/\varepsilon \lesssim 10$ account for N_e. Keep in mind that the treatment in Approx. B has a significant limitation which disregards the e's mass. As a result, the e spectra reaches unrealistic energy values below the e mass down to $E \to 0$.

A. Solutions for monochromatic e or γ

There is no exact closed form expression for the solution of the shower equations in Approx. B with the initial condition of a monochromatic e or γ of energy E_0. Rossi and Greisen proposed using the following formulae to approximate the solution:

$$n_{e(\gamma)\to e}(E_0,E,X) \;\simeq\; \left[n_{e(\gamma)\to e}(E_0,E,X)\right]_A \times p_1\left[\overline{s}\left(\frac{\varepsilon}{E_0},X\right),\frac{E}{\varepsilon}\right] \tag{34}$$

$$n_{e(\gamma)\to \gamma}(E_0,E,X) \;\simeq\; \left[n_{e(\gamma)\to e}(E_0,E,X)\right]_A \times g_1\left[\overline{s}\left(\frac{\varepsilon}{E_0},X\right),\frac{E}{\varepsilon}\right] \tag{35}$$

with $\overline{s}(x,X)$ provided by Eq. (21). The functions $p_1(s,x)$ and $g_1(s,x)$ presented in Sec. II B as part of the 'elementary solutions' to the shower equations are combined with the solution of the shower equations in Approx. A in these formulae. The solution for $E \gg \varepsilon$ matches the one found in Approx. A, although the spectra for $E \lesssim \varepsilon$ roughly resemble the shape of the 'elementary solution' corresponding to $\overline{s}(\varepsilon/E_0,X)$. It is acceptable and logical to take into account the value

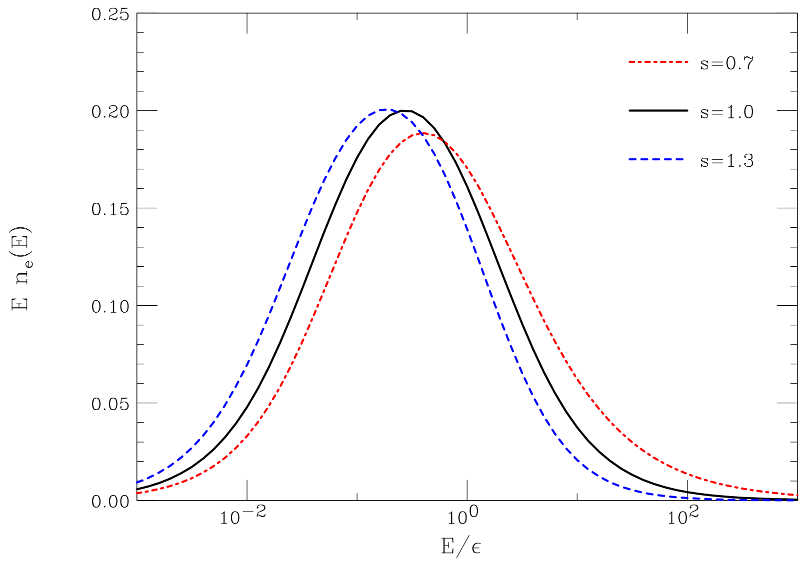

FIG. 1. The electron and photon energy distributions with the form $E\,n_e = dn_e/d\ln E$ were computed in Approx. B for three different values of s. They were estimated as: $p_1(s, E)\ E^{-s}$ and are renormalized to have a total size of one e.

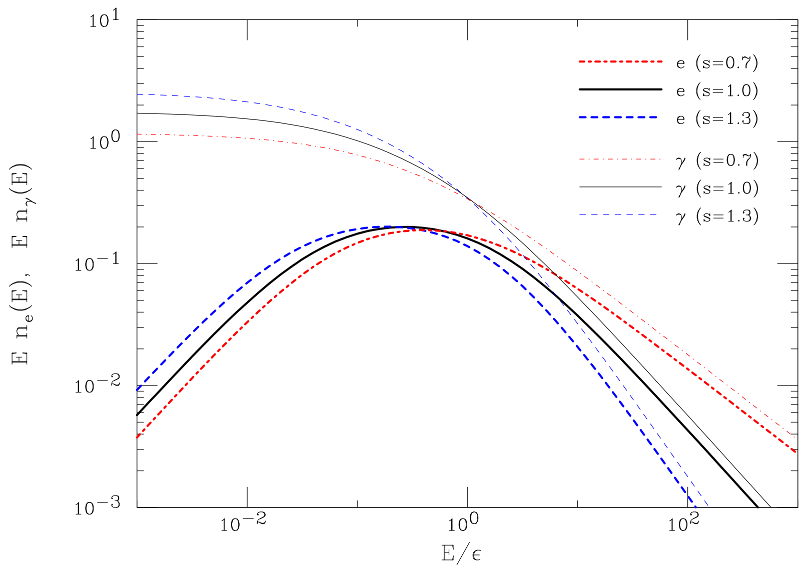

FIG. 2. The electron and photon energy distributions were computed with the form $E\,n_{e\gamma} = dn_{e,\gamma}/d\ln E$ in Approx. B for three different values of s. They were estimated as: $p(s, E)\ E^{-s}$ for e(s) $g(s, E)\ E^{-s}\,r_\gamma(s)$ for γ(s) and renormalized to have a total size of one e.

in Approx. B as the age of the shower:

$$s = \overline{s}\left(\frac{\varepsilon}{E_0}, X\right) = \frac{3\,X}{X + 2\,\ln(E_0/\varepsilon)}. \tag{36}$$

The following expression provides a good approximation of the $N_e(E_0, X)$ of the EAS computed integrating across all energies:

$$N_{\gamma(e)\to e}(E_0, X) = \frac{1}{\sqrt{2\pi}} \left[\left(\frac{E_0}{\varepsilon}\right)^s \frac{K_1(s,-s)}{s} \frac{G_{\gamma(e)\to e}(s)}{\sqrt{\lambda_1''(s)\, X}}\, e^{\lambda_1(s)\, X} \right]_{s=\bar{s}(\varepsilon/E_0, X)}, \tag{37}$$

where we have used the fact that the integration over energy is dominated by $E \sim \varepsilon$, and the result in Eq. (33). It is evident that the condition $\lambda_1(s) = 0$ which implies $s = 1$, coincides with the maximum of the size. Solution of Eq. (36):

$$X_{\max} \simeq \ln \frac{E_0}{\varepsilon}. \tag{38}$$

The following equation can be used to express energy conservation in Approx. B:

$$\int_0^{E_0} dE\; E\; n_e(E_0, E, X) + \int_0^{E_0} dE\; E\; n_\gamma(E_0, E, X) = E_0 - \varepsilon \int_0^X dX'\; N_e(E_0, X'). \tag{39}$$

The energy in the shower particles at depth X is represented on the left side of this equation, and the energy dispersed in the medium by the electrons as ionization is given by the second term on the right. Additionally, Eq. (39) suggests:

$$\varepsilon \int_0^\infty dX\; N_e(E_0, X) = E_0. \tag{40}$$

Figure. 3 displays an example of the e and γ spectra computed in Approx. A and Approx. B for a γ photon with starting energy 10^{18} eV at $X_{\max.}$. At lower energies, the two solutions diverge, but they coincide for $E \gg \varepsilon \simeq 81$ MeV. Below the critical energy, the spectra in Approx. B are significantly suppressed. Each particle type's energy is represented by the total of the areas beneath the curves. Because some of the energy has been distributed as ionization in the air, the curves of the Approx. B solution encompasses a smaller area.

According to the definition in Eq. (36), showers produced by different primaries but having the same age s in Approx. B have 'essentially' equal spectra. Figure 4, which displays the e spectra at $X_{\max}$ for showers produced by γ(s) of various energies, exemplifies this idea more clearly. Two distinct representations of the spectra are displayed. The first is of the type ($E\; dn/dE$ versus E); in this instance, the multiplicity of e(s) is proportional to the area below the curve. The spectra in the alternative format are displayed as ($E^2\; dn/dE$ versus E); in this instance, the region below the curve corresponds to the energy contained in e(s). The distributions of the highest energy particles vary, although most particles in showers of the same s have coincident spectral forms. Because high E particles make up a large portion of the energy in the shower, the evolution of an EAS with X depends not only on s but also on the EAS energy (or, equivalently, on the position $X(s)$) where the age s is attained. To summarize the findings of this section: the explicit estimation of the average evolution of solely EM showers suggests that the s parameter can be defined as,

$$s \simeq \lambda_1^{-1} \left[\frac{1}{N_e} \frac{dN_e}{dX} \right] \simeq \frac{3\,X}{X + 2\,\ln(E_0/\varepsilon)} \simeq \frac{3\,X}{X + 2\,X_{\max}}. \tag{41}$$

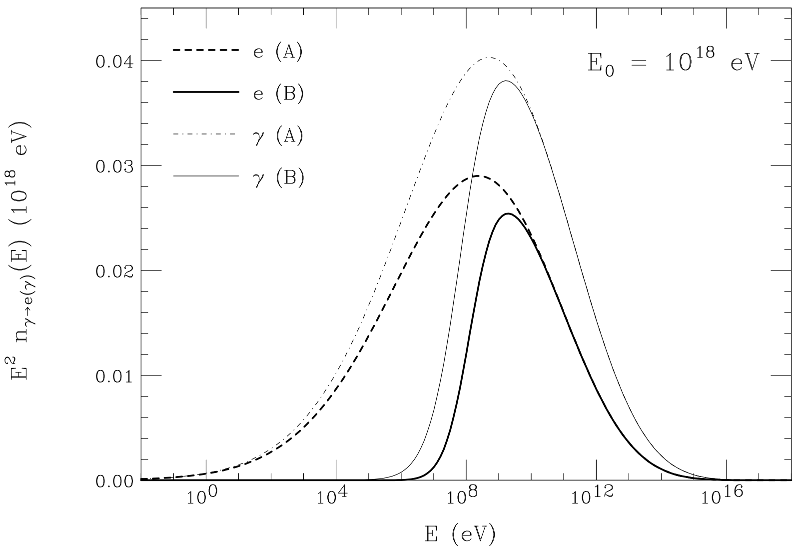

FIG. 3. The spectra of secondary es and γs in the shower produced by a primary γ with energy 10^{18} eV at shower maximum ($X = 23.7$ in radiation length unit) are compared using Approx. A and Approx. B solutions. The amount of energy carried by each particle is shown by the area beneath each curve.

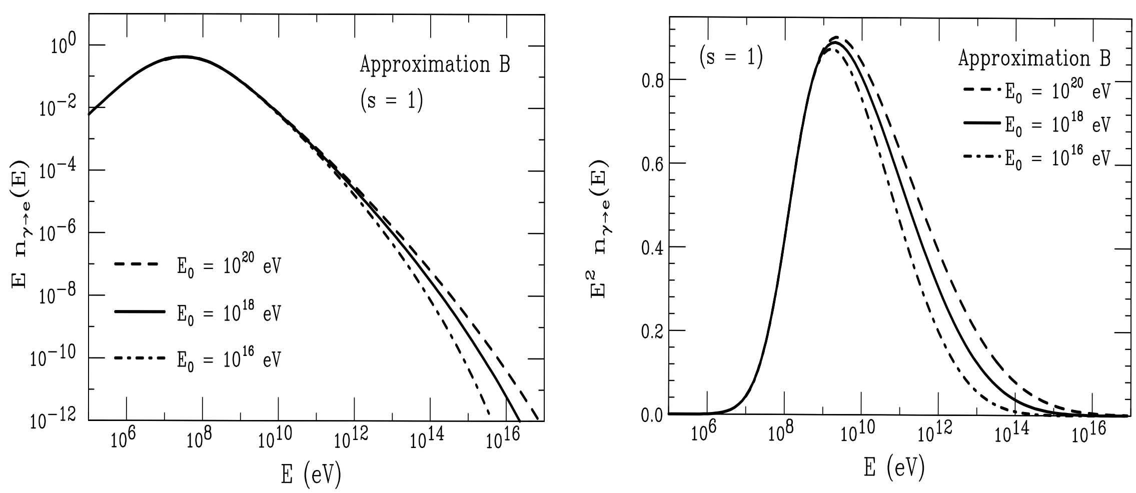

FIG. 4. The spectra of secondary e(s) of the showers produced at shower maximum ($X = 18.6$, $X = 23.7$, and $X = 27.8$ in radiation length unit) by primary γs with energies of 10^{16} eV, 10^{18} eV, and 10^{20} eV. The normalization is used so that at $E = \varepsilon = 81$ MeV, the spectra are the same. The spectra with the same age $s = 1$ are displayed in the left panel as $En(E)$ and in the right panel as $E^2n(E)$ versus E.

The spectra of e(s) and γ(s) about and below ε have the same shape in showers of the same s. At higher energies, the energy spectra are different.

IV. THE GREISEN PROFILE

Greisen [7] developed a straightforward analytical expression that appropriately describes the average longitudinal development of a purely EM shower generated by a γ or e of energy E_0:

$$N_{\text{Greisen}}(E_0, X) = \frac{0.31}{\sqrt{\ln(E_0/\varepsilon)}}\ \exp\left[X\left(1 - \frac{3}{2}\log\left(\frac{3X}{X + 2\ \ln(E_0/\varepsilon)}\right)\right)\right] \tag{42}$$

The more complicated formulation provided in Eq. (22) is practically the same as the 'Greisen Profile'. The straightforward and instructive derivation [7] of Eq. (42) necessitates the clever 'recombination' of some of the previously obtained solutions. The starting point of the calculation is the remark that the saddle point solution for the N_e [Eq. (37)] confirms the approximate validity of the relation:

$$\frac{dN_e(X)}{dX} = \lambda_1(s)\ N_e(X) \tag{43}$$

with the s given by Eq. (41). Equation (43) can now be rewritten by substituting the approximation $\overline{\lambda}_1(s)$ from Eq. (11) for $\lambda_1(s)$:

$$\frac{dN_e(X)}{dX} = \lambda_1(s)\ N_e(X) = \frac{1}{2}\left[\frac{3X}{X + 2\,X_{\text{max}}} - 1 - 3\ \log\left(\frac{3X}{X + 2\,X_{\text{max}}}\right)\right]\ N(X)\,. \tag{44}$$

This differential equation can be easily solved for the boundary condition $N(X_{\text{max}}) = N_{\text{max}}$ as follows:

$$N_e(X) = N_{\text{max}}\ e^{-X_{\text{max}}}\ \exp\left[X\left(1 - \frac{3}{2}\log\left(\frac{3X}{X + 2\,X_{\text{max}}}\right)\right)\right]. \tag{45}$$

The normalization is set by considering that the size at maximum for an EM EAS may be found by entering $s = 1$ in Eq. (37), yielding the following result:

$$N_e^{\text{max}}(E_0) = \frac{0.31}{\sqrt{\ln(E_0/\varepsilon)}}\ \frac{E_0}{\varepsilon} \tag{46}$$

where we have used

$$\frac{1}{\sqrt{2\pi}}\ \frac{G_{\gamma\to e}(1)}{\sqrt{\lambda_1''(1)}}\ K_1(1,-1) = \frac{1}{\sqrt{2\pi}}\ \frac{G_{e\to e}(1)}{\sqrt{\lambda_1''(1)}}\ K_1(1,-1) \simeq 0.31. \tag{47}$$

The final answer in Eq. (42) is obtained by substituting this result in Eq. (45). Although expressions in Eq. (37) and Eq. (42) 'look' different from one another, their numerical values are nearly identical. Equation (40) can be used to validate energy conservation and assess the accuracy of the Greisen profile solution. In the wide energy range from a few GeV to 10^{20} eV, this energy conservation criterion is satisfied to better than 4.5%.

In conclusion, the expression for the age in Eq. (5) or Eq. (41) and the Greisen profile Eq. (42) are equivalent. The shower develops with the Greisen profile Eq. (44) according to the definition of shower age in Eq. (5), and the Greisen profile implies the simple functional dependency for the age of Eq. (5). Through the mapping $\lambda_1(s)$, the Greisen profile and the 'Greisen age' Eq. (5) are the derivative and integral of one another:

$$s(X, X_{\max}) = \frac{3\,X}{X + 2\,X_{\max}} \iff N(X) =_{\text{Greisen}} (X, X_{\max}). \quad (48)$$

One could argue that the precise integration of a well-defined differential equation produces the Greisen profile. Additionally, we have learned that while the distribution of the high energy particles depends on other factors, s dictates the form of the energy spectra of the bulk of the e(s) and γ(s) in the EAS. The only additional parameter for an EM shower's average development is E_0 (or, alternatively, $X_{\max} \simeq \ln(E_0/\varepsilon)$). The overall development of an EAS depends on the high energy particle content. According to the Greisen profile, the shower has a spectrum of high energy particles at each level X that matches the shape of the development. This high energy particle content depends not only on s but also on E_0 for each s.

V. CONCLUSIONS

When analyzing CR data, the notion of the shower age might be quite helpful. The notion is fairly straightforward and may be summed up as follows: a one-to-one mapping between the X–slope λ and the E–slope s of an EAS. The fractional rate of variation of the shower size with increasing depth ($\lambda = N^{-1}\,dN/dX$) is known as the X–slope (or size slope). The integral slope of the (power law) energy spectrum of γ(s) or e(s) above the critical energy is known as the E–slope, (or energy slope). The mapping between λ and s is given by $\lambda = \lambda_1(s) \simeq (s - 1 - 3\,\ln s)/2$. The spectra of γ(s) and e(s) have a relative normalization that is also determined by s (or λ), and they have a more complex form around and below ε that is also determined by s (or λ). The fact that the founders Rossi and Greisen used analytical techniques to precisely determine the e and γ spectra that correspond to various s (or λ) several decades ago, is remarkable. The definition of s discussed here is more general and accurate than the widely used definition: $s \simeq 3\,X/(X + 2\,X_{\max})$, which is accurate only when the shower development is described by the 'Greisen profile' because it is independent of the shape of the longitudinal development of an EAS. The characteristics of hadronic interactions and the nature of particles dictate the average shape (and the variations around this average) of the longitudinal development of high energy to extremely high energy and even to UHE CR EASs. For upcoming experimental research, the observation of these shapes is a crucial topic.

All neutrino/hadron-induced showers, where the shower size is dominated by e(s), the definition of age based solely on the derivative of the shower size can be employed. This comprises showers produced by exotic primaries (such as magnetic monopoles, etc.) or showers developed by PCRs of known nature that exhibit unusual physics (or unexpected fluctuations). An intriguing line of inquiry is the search for events with peculiar longitudinal developments, such as multiple maxima or a long plateau after the depth of the shower maximum. The spectra of the EM component around and below the critical energy are probably (or at least the best feasible *a priori* assumption) controlled by s in these situations as well. There are various ways in which these concepts can be used to the study of CR observations. For instance: (i) a better reconstruction of the longitudinal profile of the shower in observations using fluorescence and/or Cherenkov light detectors can be obtained by knowing the variations of the energy spectrum of e(s) during the evolution of an EAS [9]; (ii) the reconstruction of s from the lateral density distribution of its EM component can possibly aid in the reconstruction of the energy in surface array measurements [10–12]; (iii) the redundant measurement of s (from the size longitudinal development and the lateral distribution of the EM component at the ground) can be used in hybrid measurements of the showers to test hadronic interaction models or disentangle a muon component.

[1] B. Rossi and K. Greisen, Rev. Mod. Phys. **13**, 240 (1941).
[2] J. Nishimura and K. Kamata, Progr. Theor. Phys. **6**, 93 (1958).
[3] K. Greisen, Prog. in Cosmic Ray Physics, North Holland, Co., Amsterdam, **3**, 1 (1956).
[4] M. Giller *et al.*, J. Phys. G: Nucl. Part. Phys. **30**, 97 (2004).
[5] F. Nerling, J. Blumer, R. Engel and M. Risse, Astropart. Phys. **24**, 421 (2006).
[6] D. Gora *et al.*, Astropart. Phys. **24**, 484 (2006).
[7] K. Greisen, Ann. Rev. Nucl. Part. Sci. **10**, 63 (1960).
[8] P. Lipari, Phys. Rev. D **79**, 063001 (2009).
[9] M. Unger *et al.*, Nucl. Instrum. Meth. in Phys. Res. A **588**, 433 (2008).
[10] R. K. Dey, A. Bhadra and J. N. Capdevielle, J. Phys. G **39**, 085201 (2012).
[11] R. K. Dey and S. Dam, Eur. Phys. J. Plus **131**, 402 (2016).
[12] R. K. Dey and A. Bhadra, Astro. Part. Phys. **44**, 68 (2013).